Nonlinear pulse propagation phenomena in ion-doped dielectric crystals

Gabor Demeter,[1,*] Zsolt Kis,[1] and Ulrich Hohenester[2]

[1]*Wigner Research Center for Physics, Hungarian Academy of Sciences, Konkoly-Thege Miklós út 29-33, H-1121 Budapest, Hungary*

[2]*Institut für Physik, Karl-Franzens-Universität Graz, Universitätsplatz 5, A-8010 Graz, Austria*

(Received 17 November 2011; published 19 March 2012)

We theoretically analyze pulse propagation in a medium of inhomogeneously broadened two-level quantum systems, which have a vibrational degree of freedom with respect to the center-of-mass coordinate. This system mimics local mode oscillations of rare-earth-metal-ion dopants in dielectric crystals that are coupled to electronic transitions. We show the emergence of various nonlinear optical phenomena, such as self-induced transparency or the nonlinear interaction between two pulses coupling to different electrovibrational transitions. Interaction between the pulses makes it possible to generate various Raman sidebands of the incident fields and to tune the location where they are generated. We also demonstrate controlled population transfer between electrovibrational states of the ions at specific points along the propagation axis. Similarities and differences between our results and other pulse propagation phenomena of few-level quantum systems are discussed.

DOI: 10.1103/PhysRevA.85.033819 PACS number(s): 42.50.Gy, 42.65.Dr, 42.65.Tg, 42.50.Md

I. INTRODUCTION

Coherent optical phenomena, such as self-induced transparency [1,2], photon echo [3,4], electromagnetically induced transparency, slow light [5,6], and numerous other effects, have received considerable interest in recent years. This is because they can be exploited for various applications, including efficient nonlinear field conversion, few-photon light switching, and quantum communication and quantum computing.

Among the materials used for coherent optical phenomena, rare-earth-metal-ion-doped crystals play an important role as they possess remarkably long optical coherence times [7–9]. While the microscopic theory of optical transitions in rare-earth-metal-ion-doped crystals is rather complex [10–15], typically building upon semiempirical Hamiltonians [10,16,17], it is by now well established that the low-temperature spectra are governed by sets of equidistant vibronic transitions. They arise from the electronic states of the dopant ions, which are coupled to localized vibrational modes of the ions and the surrounding lattice [18–23]. In the optical spectra the resulting vibronic sublevels are about 10–100 cm^{-1} apart. Similar to the Franck-Condon principle of natural molecules, vibrational motion of the ions is excited in conjunction with electronic excitation. This is because the potential that restrains the ion within the lattice depends on its electronic state; hence the equilibrium position and the vibrational frequency may both change with an electronic transition [12]. In contrast to natural molecules, the electronic transitions are typically inhomogeneously broadened because of strain effects.

In this paper, we study optical pulse propagation effects within a medium of inhomogeneously broadened molecule-like systems, designed to model dopant ions and their immediate surroundings within a crystal lattice. We employ a generic but simple model consisting of systems with two electronic states and a center-of-mass motion, which is assumed to take place within a pair of harmonic potentials, one for the ground and another one for the excited state (configurational coordinate model for the dopant ions in solids; see, e.g., [12,19]). The two potentials, which we consider for simplicity as one-dimensional, are displaced with respect to each other and can have different level spacings. We consider optical coupling to a set of laser pulses resonant with the different electrovibrational transitions in the resolved sideband regime. We compute the propagation of the pulses in an optically thick medium. Throughout we assume the crystal to be at low temperatures and take the initial state of the ions as the lowest vibrational level of the electronic ground state. Both intraband and interband relaxation processes are neglected.

For single pulses that are nearly resonant and not too strong, we find that the propagation is identical to that inside a medium of inhomogeneously broadened two-level systems. For the simultaneous propagation of two pulses, resonant with different electrovibrational transitions of the ions, we find that a large number of quantum states are connected in a chainwise manner, leading to a rich variety of nonlinear interactions between the two pulses. Among them are the generation of fields on various Raman sidebands of the incident radiation, the absorption of one pulse together with the amplification of the other one, and the generation of Raman sidebands at a tunable location along the propagation direction. Our results also demonstrate a controlled population transfer between electrovibrational states of the ions at specific spatial locations through coupling to the propagating pulses.

Our scheme resembles that of stimulated Raman scattering (SRS) in the transient regime [24–31], where the pulse width τ is much shorter than the dephasing time of the molecular dipole but much longer than the vibrational period associated with the Raman transition. In this regime it is possible to generate a high number of Raman sidebands. The generated modes propagate as solitary waves and are mode locked by the dynamics of the molecular polarization. The resonant coupling and the chainwise connection of the levels are the principal difference between our scheme and that of transient SRS.

Quite generally, the problem studied in this paper is closely related to several previous works on self-induced transparency, pulse matching, and solitary wave propagation in three- and five-level systems [32–37]. Indeed, in our work several

*gdemeter@rmki.kfki.hu

propagation phenomena turn out to be similar to those obtained for three-level systems, such as the analytical solutions for two-pulse propagation with an energy exchange between the pulses [32]. Nevertheless, the current system is considerably more complex since two copropagating pulses of different frequencies couple nearly resonantly to a long (infinite) ladder of chainwise connected states, which gives rise to variety of effects.

This paper is organized as follows: In Sec. II we introduce the theoretical framework underlying our analysis. The basic properties of pulse propagation are considered in Sec. III. In our system the various generated field modes have different group velocities; hence it is possible to tune the location of the interaction of the modes in the medium. This effect is discussed in Sec. IV. Finally, Raman sideband generation is studied in Sec. V. The summary and some conclusion can be found in Sec. VI.

II. THEORETICAL FRAMEWORK

In our approach we consider an ensemble of quantum systems with a ground state and an excited electronic state, each possessing a series of vibrational substates $|g,m\rangle,|e,n\rangle$ (see Fig. 1). The individual systems are defined by the Hamiltonian $\hat{H} = \hat{H}_A + \hat{H}_{AF}$, where the "atomic" Hamiltonian $\hat{H}_A$ for the ions is given by

$$\hat{H}_A = \hbar\omega_{eg}\sum_m |e,m\rangle\langle e,m| + \hbar v_g \sum_j j|g,j\rangle\langle g,j| + \hbar v_e \sum_j j|e,j\rangle\langle e,j|. \quad (1)$$

The last two terms describe the center-of-mass motion of the system in a pair of one-dimensional harmonic potentials (as we are only interested in the properties of the excited system, we have not explicitly indicated the zero-point energy of the oscillators). The energy difference between $|g,0\rangle$ and $|e,0\rangle$ is assumed to be much larger than the difference between the vibrational levels $\omega_{eg} \gg v_g, v_e$. Note that the restriction of the harmonic oscillator to a single spatial dimension is valid for systems whose optical response is governed by a single vibronic transition.

We assume that an ensemble of such molecular systems interacts with a classical electric field $E(z,t)$. Using the usual dipole and rotating-wave approximations, the interaction Hamiltonian $\hat{H}_{AF}$ is given by

$$\hat{H}_{AF} = -\hat{d}^{(+)}E^{(-)} - \hat{d}^{(-)}E^{(+)}, \quad (2)$$

where

$$\hat{d}^{(+)} = \sum_{m,n}\langle g,m|\hat{d}|e,n\rangle|g,m\rangle\langle e,n| = d_{ge}\sum_{m,n}\mathcal{F}_{m,n}|g,m\rangle\langle e,n|. \quad (3)$$

The dipole matrix elements between the various ground- and excited-state sublevels are assumed to factor into a constant matrix element $d_{eg} \in \mathbb{R}$, calculated from the electronic-state wave function, and a Franck-Condon factor $\mathcal{F}_{m,n}$. The matrix of Franck-Condon factors is given by

$$\mathcal{F}_{m,n} = \int \phi^*_{g,m}(x)\phi_{e,n}(x-D)dx, \quad (4)$$

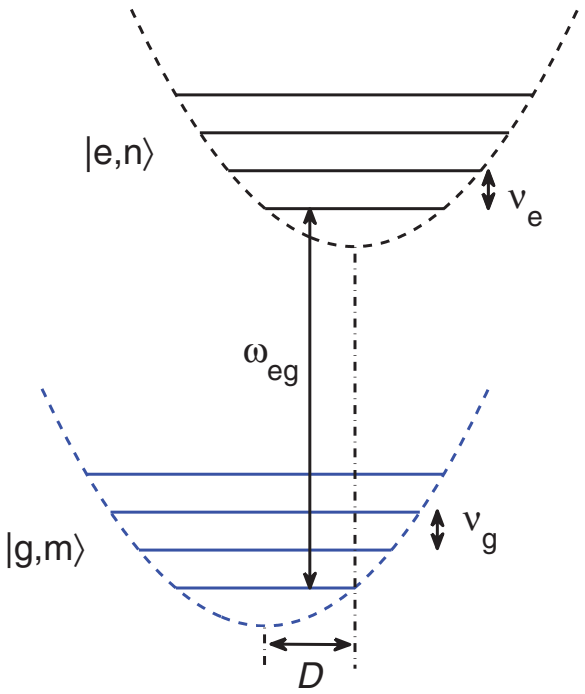

FIG. 1. (Color online) Level scheme of the considered model system. The center-of-mass motion of the ions in the harmonic potentials gives rise to a set of equidistant vibrational levels $|g,m\rangle,|e,n\rangle$ for the ground and excited electronic states with spacing v_g and v_e, respectively. The potential minima for the two electronic states are displaced by a distance D with respect to one another.

where $\phi_{g,m}$ and $\phi_{e,n}$ denote the vibrational eigenfunctions of the ground- and excited-state potentials, respectively. We assume that the displacement of the excited-state potential relative to the ground-state one is D [38] and denote the characteristic length scales of the harmonic oscillators with level spacings $v_{g,e}$ as $\xi_{g,e} = \sqrt{\hbar/Mv_{g,e}}$. Throughout we neglect the decay between different vibronic sublevels.

We describe the field $E(z,t) = E^{(+)}(z,t) + E^{(-)}(z,t)$ as a superposition of several plane waves with a constant frequency spacing,

$$E^{(+)}(z,t) = \frac{1}{2}\sum_l \varepsilon_l(z,t)e^{-i(\omega_l t - k_l z)}, \qquad \omega_l = \omega_0 + l\delta, \quad k_l = \eta\,\omega_l/c, \quad l \in \mathbb{Z}, \quad (5)$$

where the complex amplitudes $\varepsilon_l(z,t)$ vary slowly in time and space on the scale of ω_l^{-1} and k_l^{-1}, respectively, c is the speed of light in vacuum, and η is the refractive index of the host medium.

Writing the state of an ion with transition frequency ω_{eg} located at position z along the propagation direction as

$$|\psi\rangle = \sum_m a_m(z,t)e^{-im(\delta+\Delta)t+im\delta z/c}|g,m\rangle + \sum_n b_n(z,t)e^{-in\delta t+in\delta z/c}e^{-i(\omega_{eg}t-k_0 z)}|e,n\rangle, \quad (6)$$

the Schrödinger equation for the probability amplitudes a_m, b_n can easily be derived to be

$$\begin{aligned} i\partial_t a_m(z,t) &= (m\kappa_g - \Delta)a_m(z,t) - \frac{1}{2}\sum_l \Omega_l^*(z,t) \\ &\quad \times \sum_n \mathcal{F}_{m,n} b_n(z,t) e^{i(l+m-n)\delta(t-z/c)} \\ i\partial_t b_n(z,t) &= n\kappa_e b_n(z,t) - \frac{1}{2}\sum_l \Omega_l(z,t) \\ &\quad \times \sum_m \mathcal{F}^\dagger_{n,m} a_m(z,t) e^{-i(l+m-n)\delta(t-z/c)}. \end{aligned} \tag{7}$$

Here we have introduced the notation

$$\Omega_l(z,t) = \frac{d_{eg}\varepsilon_l(z,t)}{\hbar} \tag{8}$$

for the Rabi frequency of the lth pulse mode. Note that this frequency corresponds to a unit Franck-Condon factor, whereas the effective Rabi frequency for a $|g,m\rangle \rightarrow |e,n\rangle$ transition additionally involves the Frank-Condon factor according to $\Omega_{n-m}\mathcal{F}^\dagger_{n,m}$. $\Delta = \omega_{eg} - \omega_0$ is the detuning between the frequency of the $l = 0$ mode and the resonance frequency of the $0 \rightarrow 0$ vibrational transition of the ion under consideration. The differences between the vibrational levels in the ground and excited states and the frequency spacing δ of the modes are denoted by $\kappa_g = \nu_g - \delta$, $\kappa_e = \nu_e - \delta$.

When the frequency spacing of the vibronic levels is much larger than all other frequency scales, $\delta \gg \Delta, \Omega_l, \kappa_g, \kappa_e$, we can employ the usual random-phase approximation and neglect terms with $l + m - n \neq 0$ as they quickly average out in combination with the slowly varying amplitudes. In other words, we assume that the bandwidth of the pulses is much smaller than the spacing of the vibrational states, which is very reasonable considering that the latter is of the order of 10–100 cm^{-1}. Thus, for the evolution of the ions' state at a certain z in space we are left with

$$\begin{aligned} i\partial_t a_m(\Delta;z,t) &= (m\kappa_g - \Delta)a_m(\Delta;z,t) \\ &\quad -\frac{1}{2}\sum_l \Omega_l^*(z,t)\mathcal{F}_{m,m+l} b_{m+l}(\Delta;z,t), \\ i\partial_t b_n(\Delta;z,t) &= n\kappa_e b_n(\Delta;z,t) \\ &\quad -\frac{1}{2}\sum_l \Omega_l(z,t)\mathcal{F}^\dagger_{n,n-l} a_{n-l}(\Delta;z,t). \end{aligned} \tag{9}$$

These are the equations that we have to solve for an ensemble of ions with different detunings Δ and at different points along the z direction. In the equation we have now explicitly indicated the dependence on Δ. In general, the macroscopic response of the medium to the propagating fields involves a wide detuning distribution for the ions. Thus, for weak pulses the macroscopic coherence between ground- and excited-state sublevels decays rapidly due to dephasing. The ions are assumed to be initially in the $|g,0\rangle$ state, which is a valid assumption in the low-temperature case.

For the propagation of electromagnetic waves in the crystal doped with ions, we employ the slowly varying envelope approximation and arrive, after some manipulations (for details see the Appendix), at

$$\begin{aligned} \frac{\partial}{\partial z}\Omega_l(z,t') &= i\frac{k_0 d_{eg}}{2\epsilon_0\epsilon\hbar}\mathcal{P}_l(z,t') = i\alpha\sum_m \mathcal{F}_{m,m+l} \\ &\quad \times \int a_m^*(\Delta;z,t') b_{m+l}(\Delta;z,t') g(\Delta) d\Delta, \end{aligned} \tag{10}$$

where $\mathcal{P}_l(z,t')$ is the polarization corresponding to a given mode number l, k_0 is the wave number of light, $g(\Delta)$ is the spectral distribution of detunings, and $t' = t - z/v_g$ is the retarded time. (Here v_g is the group velocity in the host medium for the frequency range of the pulses; see the Appendix.) Note that in the above equation the lth mode of the field is driven only by the corresponding polarization mode. The constant $\alpha = \mathcal{N} d_{eg}^2 k_0/\epsilon_0\epsilon\hbar$ is the propagation constant for the medium, with $\mathcal{N}$ being the space density of ions. While in general a single absorption parameter cannot be defined for the propagation of the lth mode, in the case of a single pulse and the ions in state $|g,m\rangle$ initially, one recovers the well-known Beer's absorption law, where the decay parameter for the field is given by $\alpha_{\text{Beer}} = \pi\mathcal{F}^2_{m,m+l} g(0)\alpha$.

Our model calculation for the center-of-mass vibrations of the dopant ions is based on an elementary one-dimensional model for the local vibrations, while in reality the ions are embedded in a three-dimensional crystal. However, it has been shown that both heavy and light ions can have localized vibrational modes in three-dimensional host crystals (see [39,40] and references therein for an extensive review). Green's-function analysis shows that the local modes can have small linewidths (a fraction of 1 cm^{-1}), but this field is still not well understood. Our proposal assumes a pulse length in the picosecond-nanosecond range; hence a homogeneous linewidth of 0.1–0.01 cm^{-1} for the local vibrational modes is sufficiently small.

III. PROPAGATION OF PULSES

We have numerically solved Eqs. (9) and (10). The pulses entering the medium at $z = 0$ are assumed to be

$$\Omega_j(0,t) = \begin{cases} A_j \sin^2\left(\pi\frac{t-T_j}{\tau_j}\right), & t \in [T_j, T_j+\tau_j], \\ 0, & \text{otherwise}, \end{cases} \tag{11}$$

where A_j is the amplitude, T_j is the time delay, and τ_j is the temporal width of the jth pulse. In the current work, we consider at most two pulses of different modes entering the medium. The pulse lengths are assumed to be much shorter than the typical relaxation times of the excited-state sublevels and the single atom dipole relaxation time. This is necessary to justify the use of the Schrödinger equation. It does not constitute a severe restriction since excited-state lifetimes of rare-earth metals in solids can be as long as 100–1000 μs, and the homogeneous lifetime (dipole relaxation time) is of the order of 10–100 μs at 4 K. For the detunings we consider a Gaussian distribution $g(\Delta) = \exp(-\Delta^2/2\sigma_\Delta^2)/(\sigma_\Delta\sqrt{2\pi})$ with $\sigma_\Delta \gg A_j, 1/\tau_j$. Throughout this work we set $\nu_g = \nu_e = \delta$ and only consider displaced, but undistorted, potentials. It is assumed that the vibrational levels are well resolved, i.e., $\sigma_\Delta \ll \delta$. Furthermore, we use for the displacement between the two potentials $D = \xi$, which results in Franck-Condon

factors that decay fast with the difference in the numbers of vibrational excitations. In what follows, we will always use the dimensionless spatial coordinate normalized through the propagation constant, $z' = \pi g(0)\alpha z$.

A. Single pulses: Self-induced transparency

Let us first consider the propagation of a single pulse inside a medium of inhomogeneously broadened ions. When the vibrational spacing of the states is much larger than the pulse bandwidth $1/\tau_j$ (resolved sideband regime), any pulse with $l \geqslant 0$ effectively interacts with an inhomogeneously broadened medium of two-level systems. It therefore produces self-induced transparency (SIT) phenomena [1,2]. Thus it becomes completely absorbed for sufficiently weak pulses (of pulse area $\mathcal{A} = \int \mathcal{F}_{m,m+l}\Omega_l(t')dt' < \pi$), reshapes into the classical "sech" SIT solitons for stronger pulses (of pulse area $\pi < \mathcal{A} < 3\pi$), and breaks up and reshapes into multiple SIT solitons for the strongest pulses (for $\mathcal{A} > 3\pi$). On the other hand, any single pulse with $l < 0$ propagates unaffected since, with all the ions in $|g,0\rangle$, there is no transition it can excite.

B. A pair of interacting pulses

The simultaneous propagation of two pulses of different modes gives rise to a rich variety of phenomena. Previously, many interesting solutions have been found for simultaneously propagating pulses in media consisting of multilevel systems, where each field interacts with one specific transition (e.g., matched pulses for Λ or double-Λ atoms [33] or the dark coherence wave equation for Λ atoms [37]). Things are more complicated in our case since two fields of different l couple a whole set of electrovibronic states in a chainwise manner, e.g., for $l = 0$ and $l = -1$ we have $|g,0\rangle \to |e,0\rangle \to |g,1\rangle \to |e,1\rangle \to |g,2\rangle \to \ldots$. In addition, the same field interacts with several of these transitions and thus yields a whole set of different Rabi frequencies. As the two fields are able to drive the ion to successively higher vibrational states, polarizations of modes other than the original input ones are generated. These, as shown by Eq. (10), can generate new fields, i.e., Raman sidebands of the input radiation.

In the following we focus our discussion on effects that do not depend on the detailed parameter values of our model but reflect general properties of the system under study. Most importantly, since modes with $l < 0$ propagate in the unperturbed medium unaltered, the light-matter interaction will tend to drive the energy of the input pulses into these modes. (Some of the energy is inevitably absorbed by the medium, of course.) An illustrative example can be seen in Figs. 2 and 3: a pulse of mode $l = 0$ enters the medium and is followed by a $l = -1$ pulse with a delay of $T_{-1} = 1.2\tau_0$. Both pulses have the same temporal width $\tau_0 = \tau_{-1}$. Figure 2 shows the contour plot of the propagation of the two modes as a function of z' and t'/τ_0, and Fig. 3 reports the time evolution of the same modes at specific propagation distances. Upon entering the medium, the first pulse Ω_0 reshapes into the usual SIT pulse and slows down. The second pulse Ω_{-1} initially does not interact with the ions, so it propagates unaltered and finally catches up with the first pulse. When the two pulses start interacting with the same set of ions simultaneously, the first

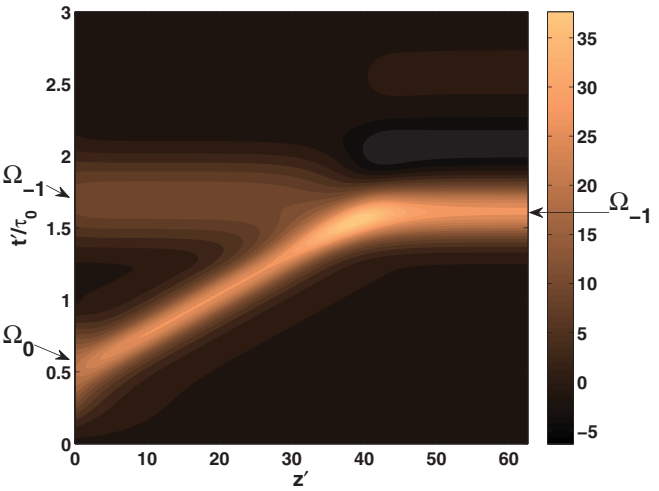

FIG. 2. (Color online) Contour plot of the sum of the two Rabi frequencies Ω_0 and Ω_{-1} as a function of z' and t' for two interacting pulses. The pulses entering the medium are labeled at $z' = 0$ on the left. The first pulse Ω_0 can be seen to propagate slowly, so the second one Ω_{-1} catches up to it. The first pulse then decays as the $l = -1$ mode becomes amplified and finally exits the medium. Parameters used for the calculation are $\tau_0 = \tau_{-1}$, $A_0 = 20/\tau_0, A_{-1} = 10/\tau_0, T_{-1} = 1.2\tau_0, \sigma_\Delta = 200/\tau_0$.

pulse is absorbed completely, while the second one reshapes and becomes amplified. The reason for this is that the first pulse excites the ions to $|e,0\rangle$ and hence creates a population inversion (on the $|e,0\rangle \to |g,1\rangle$ transition) for the $l = -1$ pulse. In the SIT soliton propagation the excitation energy then no longer returns to the $l = 0$ pulse but is transferred to $l = -1$. Eventually, the $l = 0$ pulse decays, either through a complete energy transfer to the Ω_{-1} pulse or through absorption (for an area smaller than π).

This interaction between the two pulses bears a strong resemblance to the analytic solutions derived in Ref. [32] for a medium composed of atoms with a Λ level scheme and for identical atom-field coupling parameters for the two transitions. When the atoms are prepared in one of the stable states, energy is exchanged between the two pulses, and one of the pulses completely disappears. Clearly, our case is somewhat different as we have an infinite number of chainwise connected states and the light-matter coupling is not identical for the two pulses. As a consequence, asymptotically, modes with $l < -1$ will have a finite (though small) amplitude. Despite these differences, the outcome of the interaction is quite similar. The generalized area theorem derived in Ref. [32], however, is not valid in our case.

The interaction between two pulses is more complicated when both of them can directly interact with the medium, i.e., $l \geqslant 0$. Initially, both pulses reshape into SIT pulses and slow down. Whether the two pulses can interact in the medium depends on their propagation velocities and whether the second pulse is sufficiently fast to catch up to the first one. Figure 4 shows results of a simulation where two pulses of modes $l = 0$ and $l = 1$ are injected with initial pulse areas of $\mathcal{A}_0 = \mathcal{A}_1 = 2\pi$. As the pulses interact in the medium, higher-order sidebands are created transiently (in Fig. 4 we show the $l = 2$ mode), which disappear at later times. Note that

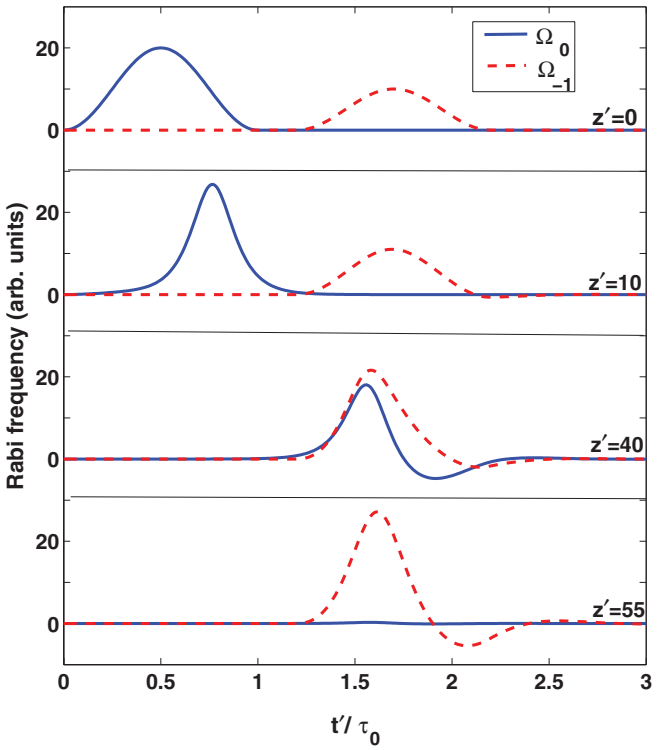

FIG. 3. (Color online) Line plots of the Rabi frequencies $\Omega_0(t')$ and $\Omega_{-1}(t')$ at specific propagation distances from the input of the medium. Parameters are the same as for Fig. 2.

high-order sidebands may propagate for quite some distance as their absorption parameters, proportional to $\mathcal{F}_{0,l}^2$, are typically small. Again, asymptotically, the energy of the pulses is transferred to modes with $l < 0$, in this case predominantly $l = -1$ and $l = -2$.

IV. SPATIALLY TUNED INTERACTION

As within the system under study certain pulses can propagate faster than others; by changing the delay between the pulses one can tune the location of the interaction within the medium at will. This could be exploited to modify the character of an output pulse leaving the doped crystal by simply tuning the time delay, which provides a resource for generating Raman sidebands with $l > 0$ or for time-resolved probing of the light-matter interaction to obtain information about the Franck-Condon factors between the vibrational states. Another interesting possibility is the transfer of population from the initial state $|g,0\rangle$ to other states, which could be used to bring the system to specific vibrational levels within selected regions of the medium, similar to the adiabatic population transfer schemes suggested in Ref. [41].

Figure 5 shows the final populations of selected levels after the interaction with two pulses with $l = 0$ and $l = 2$ as a function of the propagation distance. At specific locations all of the population is transferred to a single final state. Note that the populations are plotted for the ions that are resonant with the pulses, $\Delta = 0$. The width, as well as the location of these regions, can be flexibly tuned by changing the duration of the pulses, the delay between them, and their respective initial amplitudes.

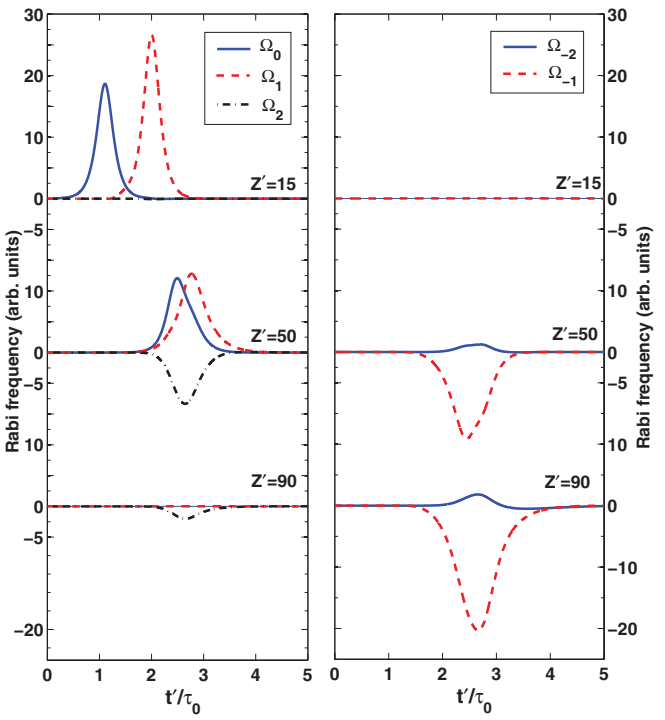

FIG. 4. (Color online) Line plots of the Rabi frequencies of several modes at specific propagation distances from the input of the medium. (left) $\Omega_0(t')$, $\Omega_1(t')$, and $\Omega_2(t')$. (right) $\Omega_{-2}(t')$ and $\Omega_{-1}(t')$. Parameters used for the calculation are $\tau_0 = \tau_1$, $A_0 = 16.1/\tau_0, A_1 = 22.8/\tau_0, T_1 = 1.2\tau_0, \sigma_\Delta = 1000/\tau_0$.

An interesting possibility derives from the fact that the displacement D between the vibrational potential minima is usually not very large, and the Franck-Condon factors for high-order sidebands of the fundamental $|0,g\rangle \rightarrow |0,e\rangle$ transition are usually small. This means that one needs a much larger amplitude to generate a pulse of $\mathcal{A} = 2\pi$ on,

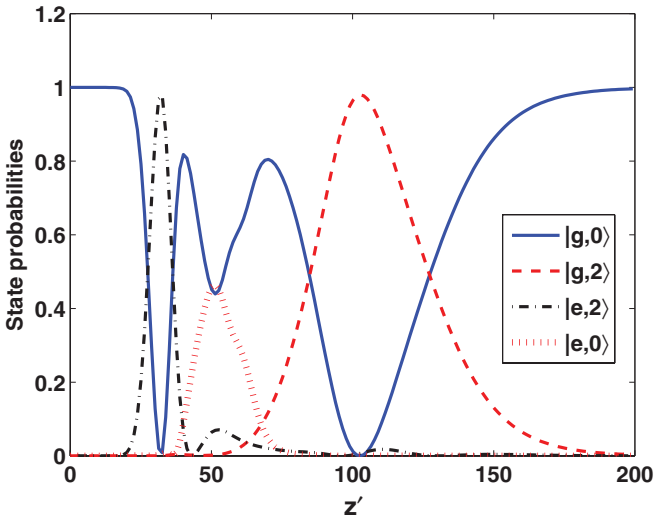

FIG. 5. (Color online) Final populations of selected states of the ions after the interaction between the two pulses has taken place as a function of propagation distance. Parameters used for the calculation are $\tau_0 = \tau_2$, $A_0 = 16.1/\tau_0, A_2 = 45.6/\tau_0, T_2 = 1.2\tau_0, \sigma_\Delta = 1000/\tau_0$. The curves refer to ions with $\Delta = 0$.

say, a $|0,g\rangle \rightarrow |4,e\rangle$ transition than the $|0,g\rangle \rightarrow |0,e\rangle$ one. Thus, a large-amplitude pulse can propagate unchanged as an $\mathcal{A} = 2\pi$ SIT pulse on a high-order sideband. When such a high-amplitude pulse interacts with a second pulse, the energy is transferred to lower-order modes, as discussed in the previous section. In the process, pulses of substantial amplitude may be transiently created in modes with $l > 0$ lying below the input mode, even pulses with $\mathcal{A} > 3\pi$. Again, by changing the delay of the second pulse, one can tune the location within the medium where the generation of these fields takes place. The significance of all this is that a pulse of $\mathcal{A} > 3\pi$ falls apart during propagation, so one cannot, in general, inject a pulse of such amplitude from the outside to any location within the medium. Nevertheless, the interaction between the pulses does provide a way to generate such pulses at any given location.

Figure 6 illustrates such a process. Two pulses with $l = 4$ and $l = 3$ enter the medium initially, with pulse areas $\mathcal{A}_3 = \mathcal{A}_4 = 2\pi$. Through the light-matter coupling, the pulse energies are transferred to lower-order sidebands until finally only modes that do not interact with the medium remain. However, there is a transient rise of field amplitudes in intermediate modes during the interaction. The top panel of Fig. 6 shows the pulse areas for the intermediate $l = 1,2,3,4$

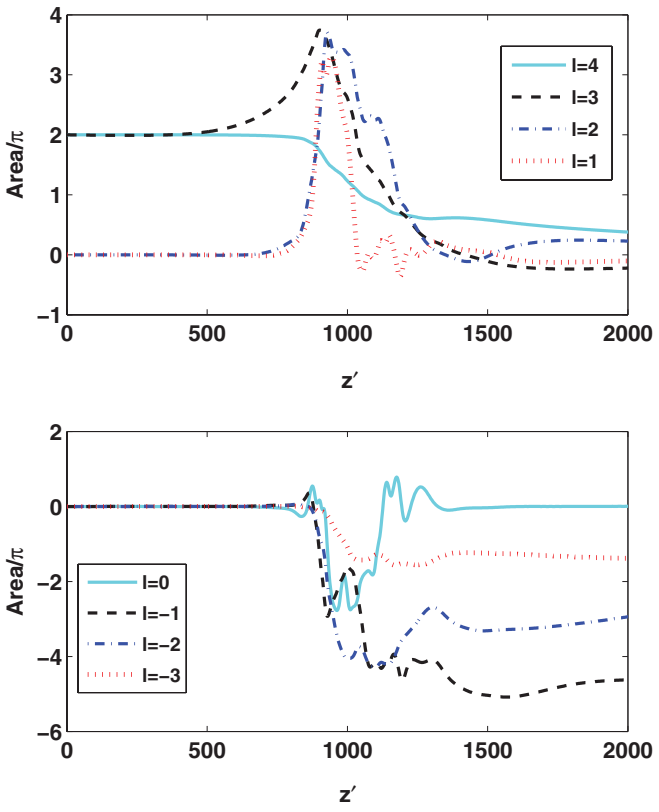

FIG. 6. (Color online) Pulse areas of specific modes l calculated using the Franck-Condon factor $\mathcal{F}_{0,l}$ as a function of propagation distance z'. (top) $\mathcal{A}_4,\mathcal{A}_3,\mathcal{A}_2$, and $\mathcal{A}_1$. (bottom) $\mathcal{A}_0,\mathcal{A}_{-1},\mathcal{A}_{-2}$, and $\mathcal{A}_{-3}$. The top panel shows intermediate modes reaching areas $\mathcal{A} > 3\pi$. Pulses like this break up during propagation, so to have one at a specific location within the medium, it must be generated there. Parameters used for the calculation are $\tau_3 = 2\tau_4$, $A_3 = 111.8/\tau_3, A_4 = 316.2/\tau_4, T_4 = 2.4\tau_4, \sigma_\Delta = 1000/\tau_0$.

modes with respect to the $|g,0\rangle \rightarrow |e,l\rangle$ transitions (i.e., calculated with the Franck-Condon factor $\mathcal{F}_{0,l}$). The areas $\mathcal{A}_3,\mathcal{A}_2$, and $\mathcal{A}_1$ can be seen to reach values close to 4π. The bottom panel shows the area of the $l = 0$ mode and the $l = -1,-2,-3$ modes. These latter ones are where the energy is finally transferred during the process. Within the transfer process some of the energy is naturally lost to the medium.

V. RAMAN SIDEBAND GENERATION

The general behavior that modes of $l \geqslant 0$ always decay while modes with $l < 0$ may amplify and finally propagate without a change is valid also when the incoming pulses are more intense. However, as more intense pulses can drive the ions into highly excited vibrational states, higher-order polarizations become sizable, and a larger portion of the energy is transferred to more distant sidebands (either permanently or transiently) as a result of the interaction. Thus, it is expected that pulses of higher amplitude can efficiently generate sidebands.

Figure 7 shows the amplitudes of the incoming and sideband modes at specific locations in the medium. From Fig. 7 it is clear that with $l = 0,-1$ modes entering the medium, the amplitudes of both the transiently created $l = 1,2$ sidebands and the output $l = -2$ sideband are considerably enhanced in comparison to the case shown in Fig. 4.

Because large area pulses break up into smaller ones while propagating, it is no longer practical to use the pulse delay to tune the location of the interaction within the medium: the interaction takes place close to the entry. Nevertheless, the

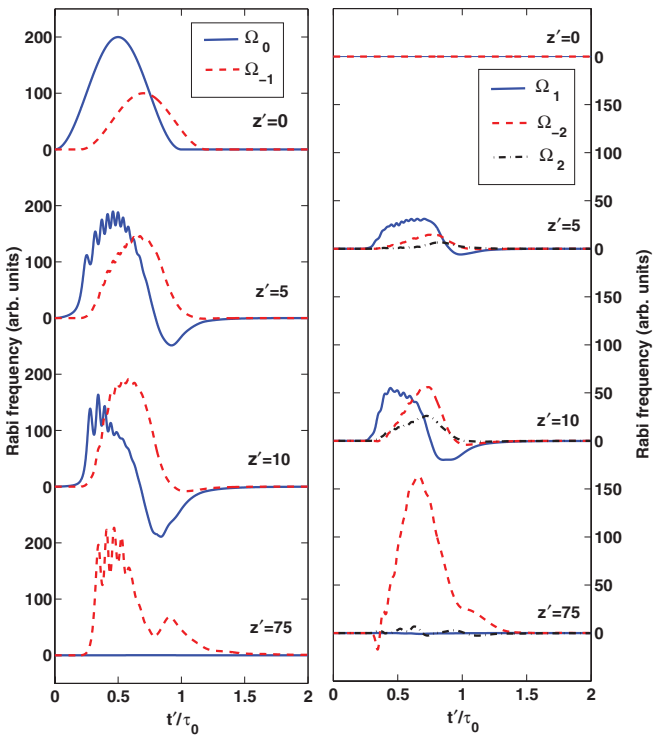

FIG. 7. (Color online) Line plots of the Rabi frequencies at specific points in space. (left) $\Omega_0(t')$ and $\Omega_{-1}(t')$. (right) $\Omega_1(t')$, $\Omega_{-2}(t')$ and $\Omega_2(t')$. Parameters used for the calculation are $\tau_0 = \tau_{-1}, A_0 = 200/\tau_0, A_{-1} = 100/\tau_0, T_{-1} = 0.2\tau_0, \sigma_\Delta = 1000/\tau_0$.

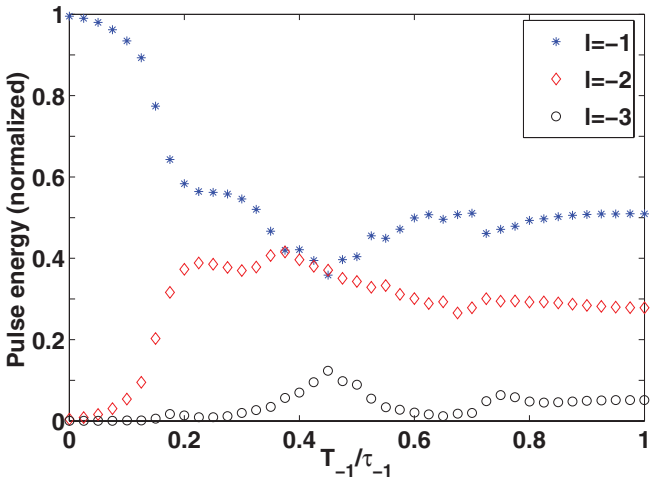

FIG. 8. (Color online) The fraction of the original input energy transferred to some specific output modes by the interaction of the two pulses as a function of the delay of the second pulse. Parameters used for the calculation are identical to those used for Fig. 7, except for the delay T_1.

delay does significantly influence how much of the overall input energy is transferred to specific sidebands. In Fig. 8 we show for different pulse delays the energy content in specific sidebands as a fraction of the original input energy after the interaction. The energy of the $l = -2$ mode shows, as a function of delay time, a rapid rise and then a slow decay, while the $l = -3$ mode exhibits a distinct peak at $T_{-1} = 0.45$. With no delay between the pulses, all of the original input energy is absorbed by the $l = -1$ mode. Note that pulse amplitudes at the input of the medium are not extremely large, corresponding to pulse areas of a few times 2π for both input modes.

VI. SUMMARY AND OUTLOOK

We have presented a numerical study of pulse propagation phenomena in a medium of two-level quantum systems, which have a vibrational degree of freedom with respect to the center-of-mass coordinate. The system is intended as a simple model for ion-doped dielectric crystals where localized oscillation modes are excited in conjunction with electronic excitation. When two pulses resonant with different electrovibrational transitions propagate in the medium simultaneously, the pulses couple a large number of electrovibrational states in a chainwise manner. This, in turn, results in strong nonlinear interactions between the pulses.

We have analyzed the simultaneous propagation of two pulses under several conditions. First, we have considered the injection of pulse pairs with several different frequencies and have shown that the nonlinear light-matter interaction tends to transfer the pulse energies to low-order Raman sidebands of the fundamental frequency. These Raman pulses propagate without further amplification inside the medium. As numerous Raman sidebands of the input radiation can be generated at least transiently, the properly chosen time delay between the two pulses can be used to release energy into these sidebands at a tunable location along the propagation direction. Using the same principle, it is also possible to generate population transfer between specific electrovibrational states at certain locations within the medium. While the phenomena occurring for the propagation of two pulses are fairly complex, in several cases similarities to propagation phenomena derived for much simpler three- and five-level systems exist, which can be used to interpret our results.

The outcome of the interaction between pulses depends upon a number of parameters, namely, input pulse mode numbers, amplitudes, temporal lengths, and delays. Thus in case of specific applications a parameter optimization will be needed in order to, e.g., maximize the energy transferred to a specific Raman sideband.

ACKNOWLEDGMENTS

This work has been supported by the Austrian-Hungarian Bilateral Project AT-2/2008. The financial support from the Janos Bolyai Research Fellowship of the Hungarian Academy of Sciences is gratefully acknowledged by G. Demeter and Z. Kis. This work has been funded by the Research Fund of the Hungarian Academy of Sciences (OTKA) under Contracts No. F67922 and No. K83390.

APPENDIX

In this Appendix we provide the details for deriving Eq. (10). Our starting point is the wave equation for the propagation of electromagnetic waves in the crystal doped with ions, which in the slowly varying envelope approximation reads

$$\sum_l k_l e^{-i(\omega_l t - k_l z)} \left(\frac{\partial \varepsilon_l(z,t)}{\partial z} + \frac{1}{v_{g,l}} \frac{\partial \varepsilon_l(z,t)}{\partial t} \right) = -i\mu_0 \frac{\partial^2 P^{(+)}(z,t)}{\partial t^2}, \tag{A1}$$

where $v_{g,l} = \partial\omega_l/\partial k_l$ is the group velocity for the lth mode with $k_l = \eta\,\omega_l/c$. The frequency-dependent refractive index η is defined through the relation $\epsilon \equiv \eta^2 = 1 + \chi(\omega)$ ($\chi(\omega)$ is the linear susceptibility of the host medium; see [26]). In the following it is assumed that the frequency spread of the modes is small, so that η can be evaluated at ω_0, which implies that all the group velocities $v_{g,l}$ are the same v_g. The positive frequency part of the macroscopic polarization $P^{(+)}(z,t)$ on the right-hand side of Eq. (A1) is entirely due to the response of the ions to the fields and is defined by

$$P(z,t) = P^{(+)}(z,t) + P^{(-)}(z,t) = \mathcal{N} \int \langle \hat{d} \rangle g(\Delta) d\Delta \tag{A2}$$

so that

$$P^{(+)}(z,t) = \mathcal{N} d_{eg} \int \sum_{m,l} \mathcal{F}_{m,m+l} a_m^*(\Delta; z,t) b_{m+l}(\Delta; z,t) \times e^{-i(\omega_l t - k_l z)} g(\Delta) d\Delta. \tag{A3}$$

In this expression $\mathcal{N}$ is the space density of the ions, and $g(\Delta)$ is the spectral distribution of the detunings of the inhomogeneously broadened ensemble. Similarly to the

electric field, we can write the polarization as a superposition of equidistant modes:

$$P^{(+)}(z,t) = \frac{1}{2}\sum_l \mathcal{P}_l(z,t)e^{-i(\omega_l t - k_l z)}, \tag{A4}$$

with

$$\mathcal{P}_l(z,t) = 2\mathcal{N}d_{eg}\int \sum_m \mathcal{F}_{m,m+l}a_m^*(\Delta;t) \times b_{m+l}(\Delta;t)g(\Delta)d\Delta. \tag{A5}$$

After taking the second derivative of Eq. (A3) with respect to time, inserting the leading-order term into Eq. (A1), and rewriting the equation using the retarded time $t' = t - z/v_g$, we obtain

$$\sum_l k_l e^{-i\omega_l t'}\frac{\partial}{\partial z}\varepsilon_l(z,t') = i\frac{\mathcal{N}d_{eg}}{\epsilon_0\epsilon}\sum_{m,l}k_l^2\int \mathcal{F}_{m,m+l}a_m^*(\Delta;z,t')b_{m+l}(\Delta;z,t') \times e^{-i\omega_l t'}g(\Delta)d\Delta. \tag{A6}$$

As described above, we can replace k_l with k_0 in the equation. This equation is strictly valid for the sum of the field components. However, because amplitudes vary little on the time scale of $1/\omega_l$, to an excellent approximation, it is valid for each l separately, and Eq. (A6) can be cast to the final form of Eq. (10).

[1] S. L. McCall and E. L. Hahn, Phys. Rev. **183**, 457 (1969).
[2] L. Allen and J. H. Eberly, *Optical Resonance and Two-Level Atoms* (Dover, New York, 1978).
[3] N. A. Kurnit, I. D. Abella, and S. R. Hartmann, Phys. Rev. Lett. **13**, 567 (1964).
[4] I. D. Abella, N. A. Kurnit, and S. R. Hartmann, Phys. Rev. **141**, 391 (1966).
[5] S. E. Harris, J. E. Field, and A. Imamoglu, Phys. Rev. Lett. **64**, 1107 (1990).
[6] M. Fleischhauer, A. Imamoglu, and J. P. Marangos, Rev. Mod. Phys. **77**, 633 (2005).
[7] R. M. Macfarlane, J. Lumin. **100**, 1 (2002).
[8] M. K. Kim and R. Kachru, Phys. Rev. B **40**, 2082 (1989).
[9] R. W. Equall, R. L. Cone, and R. M. Macfarlane, Phys. Rev. B **52**, 3963 (1995).
[10] B. G. Wybourne, *Spectroscopic Properties of Rare Earths* (Interscience, New York, 1965).
[11] A. A. Kaplyanskii and R. M. Macfarlane, *Spectroscopy of Solids Containing Rare Earth Ions* (North-Holland, Amsterdam, 1987).
[12] B. Henderson and G. F. Imbusch, *Optical Spectroscopy of Inorganic Solids* (Oxford Science Publications, Oxford, 2006).
[13] *Spectroscopic Properties of Rare Earths in Optical Materials*, Springer Series in Materials Science, edited by G. Liu and B. Jacquier (Springer, Berlin, 2005).
[14] J. García Solé, L. E. Bausá, and D. Jaque, *An Introduction to the Optical Spectroscopy of Inorganic Solids* (Wiley, Hoboken, NJ, 2005).
[15] B. Henderson and R. H. Bartram, *Crystal-Field Engineering of Solid-State Laser Materials* (Cambridge University Press, Cambridge, 2000).
[16] H. M. Crosswhite and H. Crosswhite, J. Opt. Soc. Am. B **1**, 246 (1984).
[17] W. T. Carnall, G. L. Googman, K. Rajnak, and R. S. Rana, J. Chem. Phys. **90**, 3443 (1989).
[18] M. Wagner and W. E. Bron, Phys. Rev. **139**, A223 (1965); W. E. Bron and M. Wagner, *ibid*. **139**, A233 (1965).
[19] T. H. Keil, Phys. Rev. **140**, A601 (1965).
[20] K. F. Renk and J. Deisenhofer, Phys. Rev. Lett. **26**, 764 (1971).
[21] G. K. Liu, X. Y. Chen, and J. Huang, Mol. Phys. **101**, 1029 (2003).
[22] G. K. Liu, X. Y. Chen, N. M. Edelstein, M. F. Reid, and J. Huang, J. Alloys Compd. **374**, 240 (2004).
[23] M. Karbowiak, A. Urbanowicz, and M. F. Reid, Phys. Rev. B **76**, 115125 (2007).
[24] A. P. Hickman, J. A. Paisner, and W. K. Bischel, Phys. Rev. A **33**, 1788 (1986).
[25] J. R. Ackerhalt and P. W. Milonni, Phys. Rev. A **33**, 3185 (1986).
[26] A. P. Hickman and W. K. Bischel, Phys. Rev. A **37**, 2516 (1988).
[27] A. E. Kaplan, Phys. Rev. Lett. **73**, 1243 (1994).
[28] A. E. Kaplan and P. L. Shkolnikov, J. Opt. Soc. Am. B **13**, 347 (1996).
[29] L. L. Losev and A. P. Lutsenko, Opt. Commun. **132**, 489 (1996).
[30] E. Sali, K. J. Mendham, J. W. G. Tisch, T. Halfmann, and J. P. Marangos, Opt. Lett. **29**, 495 (2004).
[31] H. Matsuki, K. Inoue, and E. Hanamura, Phys. Rev. B **75**, 024102 (2007).
[32] B. D. Clader and J. H. Eberly, Phys. Rev. A **76**, 053812 (2007).
[33] F. T. Hioe and R. Grobe, Phys. Rev. Lett. **73**, 2559 (1994).
[34] R. Grobe, F. T. Hioe, and J. H. Eberly, Phys. Rev. Lett. **73**, 3183 (1994).
[35] E. Cerboneschi and E. Arimondo, Phys. Rev. A **54**, 5400 (1996).
[36] V. V. Kozlov and J. H. Eberly, Opt. Commun. **179**, 85 (2000).
[37] J. H. Eberly and V. V. Kozlov, Phys. Rev. Lett. **88**, 243604 (2002).
[38] J.-L. Chan, J. Mol. Spectrosc. **232**, 102 (2005).
[39] R. J. Elliott, J. A. Krumhansl, and P. L. Leath, Rev. Mod. Phys. **46**, 465 (1974).
[40] A. S. Barker Jr. and A. J. Sievers, Rev. Mod. Phys. **47**, S1 (1975).
[41] J. R. Csesznegi, B. K. Clark, and R. Grobe, Phys. Rev. A **57**, 4860 (1998).